High-Field EPR Study of Carotenoid$^{\bullet+}$ and the Angular Orientation of Chlorophyll $z^{\bullet+}$ in Photosystem II

Peter Faller, A. William Rutherford, and Sun Un*

Département de Biologie Cellulaire et Moléculaire, Section de Bioénergétique, CNRS URA 2096, CEA Saclay, F-91191 Gif-sur-Yvette, France

Received: July 31, 2000; In Final Form: September 13, 2000

The carotenoid (Car$^{\bullet+}$) and chlorophyll *z* cation ($Chl_Z^{\bullet+}$) radicals in hydroxylamine treated PSII membranes from spinach were studied by 285 GHz high-field EPR spectroscopy. Car$^{\bullet+}$ was generated by 5 K illumination in the magnet. The spectrum was characterized by a g-tensor, the principal values of which were 2.00322, 2.00252, and 2.00211. The spectrum of the $Chl_Z^{\bullet+}$ generated by illumination at 198 K was clearly different from the Car$^{\bullet+}$, showing less resolution. The g-values were 2.00308, 2.00253, and 2.00216. An identical $Chl_Z^{\bullet+}$ spectrum was obtained when the sample exhibiting the Car$^{\bullet+}$ spectrum was dark-adapted at 198 K. This observation is consistent with the electron transfer from Chl_Z to Car$^{\bullet+}$ that occurs upon raising the temperature as proposed earlier [Hanley et al., *Biochemistry,* **1999,** *38,* 8189]. The spectra of the one-dimensional oriented samples were obtained to determine the angular orientation of $Chl_Z^{\bullet+}$. If one assumes that the g-tensor of the Chl_Z cation radical is oriented similar to the well-characterized bacteriochlorophyll *a*, the data show that the ring plane of $Chl_Z^{\bullet+}$ is oriented perpendicular to the membrane plane.

Introduction

Using optical and EPR spectroscopy, it has recently been shown that the cationic β-carotenoid radical (Car$^{\bullet+}$) is generated in plant Photosystem II (PSII) upon illumination at low temperature ($\leq$ 20 K) in near stoichiometric quantities.[1] Upon warming, the signal changes to that of a chlorophyll radical[1] known as chlorophyll *z* ($Chl_Z^{\bullet+}$).[2,3] The presence of these signals has been interpreted in terms of an alternative electron-transfer pathway $Chl_Z \rightarrow Car \rightarrow P680^{\bullet+}$.[1] Although it is difficult to distinguish between these two radicals using conventional 9 GHz continuous-wave EPR (cw-EPR), pulse methods can readily do so based on differences in electron−nuclear hyperfine couplings.[4] In this work we have carried out high magnetic field EPR at 285 GHz and 10.5 T. The high-field EPR spectra of the PSII chlorophyll *z* radical[5] and the in vitro canthaxanthin,[6] a related carotenoid, have been previously studied. These studies indicate that the high-field EPR spectra of the catonic Chl_Z and carotenoid radicals should be distinguishable based on g-values. In addition, relative quantification of the different radicals using high-field EPR should be more straigthforward than using either 9 GHz cw or pulse methods.

The g-tensor for the Chla$^{\bullet+}$ cation radical has been calculated using INDO/SP[7] and ZINDO.[8] Both calculations predict a tilt of approximately 10° in the g_z direction with respect to the ring-plane perpendicular direction. The measured tilt for the bacteriochlorophyll *a* cation radical is 23°.[9] Knowledge of the orientation of the g-tensor with respect to the molecular frame provides a means for determining the orientation of the molecular ring-plane with respect to the membrane plane.

By using the inherent high resolution of high-field EPR in combination with 1D-oriented samples and knowledge of the g-tensor orientation, it is possible to determine directly the orientation of a radical with respect to the axis of orientation. In the absence of a high-resolution structure, this method can provide important structural information of radicals. Although several spectroscopical studies of $Chl_Z^{\bullet+}$ have been reported,[4,5,10−12] no information regarding its angular orientation is available. Successful determination of several radical cofactor orientations in PSII by this method have been reported.[13,14]

Materials and Methods

Sample Preparation. PSII-enriched membranes from spinach were prepared essentially by the method in ref 15 with the modifications described in ref 16. Mn was depleted from PSII by incubating the membranes (1 mg of Chl /ml) at 0° for 15 min in roomlight in the presents of 2 mM freshly made NH_2-OH, then the sample was transferred to complete darkness, where the NH_2OH concentration was increased to 4 mM and incubated again for 30 min at 0°. The membranes were then pelleted by centrifugation and washed 5 times in a buffer containing 5 mM $MgCl_2$, 10 mM NaCl, 1 mM EDTA, 50 mM MES, pH 6.3, by successive resuspension and centrifugation steps in order to remove NH_2OH. The final pellet was suspended in 15 mM NaCl, 0.3 M sucrose, 50mM MES, pH 6.5, 5 mM $K_3Fe(CN)_6$. All of the washing steps described above were done in total darkness. The samples for the powder spectrum were incubated for 10 min in 0.5% β-dodecyl maltoside in order to reduce the light scattering.

Oriented Samples. To prepare the orientated samples, the Mn-depleted PSII membranes were first washed twice in 50 mM MES, pH 6.5, 5 mM $K_3Fe(CN)_6$, and then painted onto plastic films and dried in a 90% humidity atmosphere at 4°, all done in total darkness to avoid TyrD oxidation. In this work, EPR spectra were recorded for two different orientations of the plastic film with respect to the magnetic field. The plastic sheets were mounted perpendicular and parallel to the magnetic field in two different tubes.

High-Field EPR Spectroscopy. The 10 T 285 GHz high-field EPR spectrometer has been previously described.[17] Samples

* Corresponding author. Fax: ++33 (0)1 69 08 87 17, e-mail: sun@ozias.saclay.cea.fr.

10.1021/jp0027344 CCC: $19.00 © 2000 American Chemical Society
Published on Web 11/08/2000

were loaded in the dark at 77 K. Sample illumination with white light at 5 K was achieved using a Flexilux fiber optic illuminator (150 W), the output of which was directed at the microwave output waveguide window. The light was carried via the microwave waveguide to the sample in the cryostat. All spectra were obtained with 4 to 5 G field modulation. All spectra were taken under nonsaturating conditions. The absolute accuracy in g-values was $\pm 1 \times 10^{-4}$. The relative accuracy, the difference in g-values of any two points of a given spectrum, was better than 2×10^{-5}. The presence of the tyrosine-D signal (see below) provided an effective internal standard. The g-values of the $TyrD^{\bullet+}$ calibrated using a manganese-doped magnesium oxide standard are 2.00756, 2.00432, and 2.00215.[14] Using the $TyrD^{\bullet+}$ resonances as standards, it was possible to compare g-values from different spectra to within 5×10^{-5}.

Simulations. Only the electron Zeeman interaction was included in the powder pattern simulations. No explicit hyperfine interactions were included. The lack of resolved hyperfine interactions either at 0.3 or 10 T justified this exclusion. Anisotropic line width contributions, due to unresolved hyperfine anisotropy, were included using a broadening tensor, the principal directions of which were coincident with the g-tensor. The spectra were fitted using conjugate gradient minimization[18] of the root-mean-squared difference between simulation and experimental spectrum.

Density-Functional Calculations. The geometries of the various cationic polyene radicals were optimized using the semiempirical method MNDO implemented in MOPAC6.0.[19] The resulting optimized structures deviated from strict C_2 symmetry. These deviations were not significant and were averaged in order to preserve the C_2 symmetry of the polyene radicals. The resulting symmetrized structures were used in subsequent density-functional calculations. The g-tensors were determined using the ZORA formalism in conjunction with frozen-core potentials and all-electron triple-ζ basis as implemented in ADF1999.02.[20,21]

Results

Figure 1B shows results of 5 K illumination of hydroxylamine treated PSII membranes. At such low temperature conditions, $Car^{\bullet+}$ is produced in essentially stiochiometric amounts with a negligible amount of $Chl_Z^{\bullet+}$.[1,4] Before illumination (Figure 1A), weak resonances arising from $TyrD^{\bullet+}$ and $P700^{\bullet+}$ were observed. Superimposed on the dark spectrum is a $P700^{\bullet+}$ spectrum obtained by chemically oxidized P700 in PSI with 5mM $K_3Fe(CN)_6$. The $TyrD^{\bullet+}$ is due to incomplete reduction of TyrD by hydroxylamine, whereas the $P700^{\bullet+}$ is from a small PSI contamination in the PSII membranes. Although both signals occur in the same region as the $Car^{\bullet+}$ and the $Chl_Z^{\bullet+}$, they did not interfere with the analysis due to their low intensities. After 30 min of illumination at 5 K, a signal appears with g-values of 2.00322, 2.00252, and 2.00211 (Table 1). The spectrum of this putative carotenoid radical was best simulated by including anisotropic broadening. When an isotropic broadening was used, the fit was slightly poorer; however, the g-values were within 0.00005 of the values obtained using anisotropic broadening.

The sample illuminated at 5 K was then incubated at 198 K (solid CO_2/ethanol bath) for 20 min in the dark. The sample was reintroduced into the cryostat which was pre-cooled to 80 K. The 5 K spectrum of the 198 K incubated spectrum is shown in Figure 1C and is identical to the $Chl_Z^{\bullet+}$ spectrum (see below). The $Chl_Z^{\bullet+}$ resonance was clearly more readily saturable than $Car^{\bullet+}$, $P700^{\bullet+}$, and $TyrD^{\bullet+}$ resonances. Hence lower microwave power was used to obtain nonsaturated spectra. The spectra shown in Figure 1A, B, and C, which were obtained on the same sample, were scaled to take into account the number of scans and microwave power. After scaling the spectra in this manner, the g_Y portion of the residual $TyrD^{\bullet+}$ at 2.00432 in

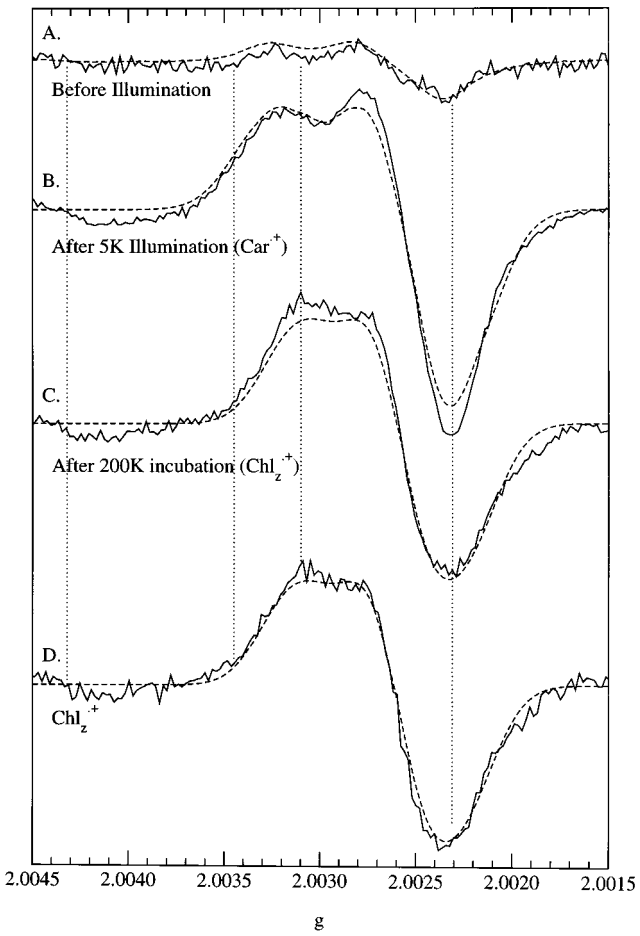

Figure 1. High-field EPR spectra (285 GHz) of hydroxylamine-treated PSII membrane samples 0.3 M sucrose, 15 mM NaCl, 50 mM MES, pH 6.5, 5 mM $K_3Fe(CN)_6$. Spectra 1A, 1B, and 1C are taken from the same sample at 5 K during a sequence of treatments and were scaled to take into account the number of scans and microwave power. A: Spectrum (1 scan) of dark-adapted PSII membranes (before illumination). Weak resonances arising from $TyrD^{\bullet+}$ and $P700^{\bullet+}$ were observed. Superimposed on the dark spectrum is a $P700^{\bullet+}$ spectrum obtained by chemically oxidizing P700 in PSI with 5 mM $K_3Fe(CN)_6$. The $TyrD^{\bullet+}$ is due to incomplete reduction of TyrD by hydroxylamine, whereas the $P700^{\bullet+}$ derives from a small PSI contamination in the PSII enriched membranes. B: the solid line is the spectrum (4 scans) measured after illumination in the magnet at 5 K for 30 min and is assigned to the $Car^{\bullet+}$. The dotted line represents the simulated spectrum. C: the solid line shows the spectrum (10 scans) of PSII membranes after illumination at 5 K for 30 min (stage of spectrum B), annealing to 198 K for 20 min in the dark and cooling back down to 5 K. The spectrum is assigned to $Chl_Z^{\bullet+}$. The dotted line represents the simulated spectrum. D: Spectrum (4 scans) at 12 K of $Chl_Z^{\bullet+}$ generated after illumination at 198 K (solid CO_2/ethanol bath).

TABLE 1: G-values of Different Carotenoid and Chlorophyll Radicals

	g-values			line widths (mT)		
β-carotene	2.00322	2.00252	2.00211	1.7	1.5	1.7
canthaxanthin[a]	2.0032	2.0023	2.0023	1.4	1.4	1.4
Chl_Z	2.00308	2.00253	2.00216	1.3	0.9	1.3
Chl_Z[b]	2.00304	2.00252	2.00213			
Chla[c]	2.00329	2.00275	2.00220	1.0	0.6	1.2

[a] From ref 6. [b] Ref 5. [c] Ref 8 (extracted).

TABLE 2: ZORA Calculated g-Values for Series of Polyenes

ethylene	2.00409	2.00237	2.00217
butadiene	2.00387	2.00255	2.00216
hexatriene	2.00380	2.00258	2.00215
octatetraene	2.00379	2.00259	2.00215
decapentaene	2.00377	2.00260	2.00214
3,7-dimethyl-decapentaene	2.00375	2.00264	2.00214
5,6-trans-decapentaene	2.00373	2.00261	2.00215

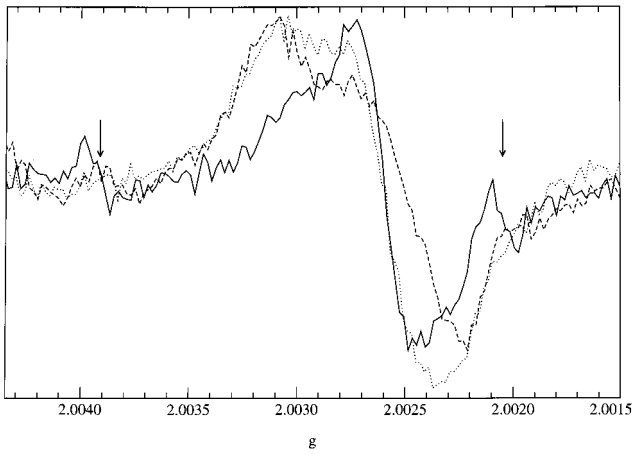

Figure 2. High-field EPR spectra (285 GHz) of $Chl_Z^{\bullet+}$ in PSII after illumination at 198 K. Dotted line: powder spectrum. Dashed line: orientation axis is parallel with the magnetic-field. Solid line: orientation axis is perpendicular to the magnetic-field. The arrows indicate the lines due to a slight Mn^{2+} contamination.

Figure 1B and C has the same amplitude. This indicates that the scaling is correct, because TyrD is not expected to undergo electron transfer at the temperatures that were used.[1] About 20% of total intensity in the 2.0035−2.0015 region was lost during incubation. A similar loss of intensity was measured by X-band EPR. This has been ascribed to the charge recombination between $Car^{\bullet+}$ and Q_A^-.[1]

As a comparison, hydroxylamine treated PSII membranes were illuminated at 198 K (solid CO_2/ethanol bath) to generate the Chl_Z radical cation.[2,3,1] Figure 1D is the high-field EPR spectrum of $Chl_Z^{\bullet+}$ taken at 12 K under nonsaturating conditions. The $Chl_Z^{\bullet+}$ spectrum was clearly different from that of the carotenoid radical, showing less resolution apparently due a lower g_X value. This was verified by simulation (Figure 1 and Table 1). The g-values (Table 2) of the Chl_Z cation radical were found to be 2.00308, 2.00253, and 2.00216, which were in good agreement with those previously reported.[5]

High-field EPR spectra of $Chl_Z^{\bullet+}$ from 1-dimensionally oriented samples were also obtained and are shown in Figure 2. When the plane of plastic films is perpendicular to the magnetic-field (Figure 2, solid-line), the spectrum was dominated by a feature which had a zero-crossing at the $Chl_Z^{\bullet+}$ g_Y value. When the films were rotated by 90° (Figure 2, dashed-line), the spectrum was broader, covering the full range of the powder $Chl_Z^{\bullet+}$ (Figure 2, dotted-line) with reduced intensity in the g_y region. These one-dimensionally oriented $Chl_Z^{\bullet+}$ spectra were simulated (results not shown) in a manner identical to those previously reported for Tyr-D, semiquinone, and pheophytin radicals.[14] A 20° distribution in the orientation angles was included in the calculation, as well as the g-values obtained from the powder spectrum. The orientation of the $Chl_Z^{\bullet+}$ g_z direction relative to the membrane plane was 19°, and the g_x 30°.

Discussion

When the plastic film plane of a one-dimensionally oriented sample is perpendicular to the applied magnetic-field, the spectrum is essentially like that of a single-crystal. In the ideal case, a single sharp resonance at the effective g-value corresponding to the specific orientation of the magnetic-field relative to the *g*-axis system is observed. Hence, even without the benefit of simulations, it is clear that the $Chl_Z^{\bullet+}$ g_y direction is approximately perpendicular to the membrane plane. Simulations confirm this qualitative analysis. A 20° distribution was included for both orientation angles. Since such a large distribution was required to obtain good fits of the Tyr-D, semiquinone, and pheophytin radical data, we have argued that this distribution represents disorder in orientation of the membrane fragments.[14] We therefore have included it for the $Chl_Z^{\bullet+}$ simulations.

The orientation of the g-axis with regard to a Chl-a molecule is not known. The g-tensor of a bacteriochlorophyll *a* molecule has been fully analyzed using the bacteriochlorophyll *a* half of the heterodimeric special-pair in a HL mutant of the *Rhodobacter sphaeriodes*.[9] In this case the g-values are 2.00299, 2.00264, and 2.00229. With the exception of a isotropic shift of +0.00002, these values are close to those of $Chla^{\bullet+}$. The g_x component of the bacteriochlorophyll $a^{\bullet+}$ is directed along the nitrogens of ring I and ring III, and the g_y component along the nitrogens of ring II and ring IV. The g_Z direction is tilted by 23° from the ring-plane normal. Within the bacterial reaction center, the ring-plane normal of the special-pair is essentially perpendicular to the membrane plane where the membrane-normal is defined by the vector connecting the average position of the magnesium ions of the special pair to the non-heme iron. Therefore, the g_Z direction of the special pair is 23° with respect to the membrane plane, compared to 19° measured for $Chl_Z^{\bullet+}$. If it is assumed that the $Chl_Z^{\bullet+}$ g-tensor is oriented similar to that in bacteriochlorophyll *a*, then our results indicate that the $Chl_Z^{\bullet+}$ ring-plane is also nearly perpendicular to the membrane.

The measured g-values for the $Car^{\bullet+}$ in PSII are distinct from those obtained for $Chl_Z^{\bullet+}$ (Figure 1B and D). These carotenoid g-values are also measurably different from those measured by Knonovalova and co-workers for the canthaxanthin radical.[6] Although the g-anisotropy, as defined by $|g_X - g_Z|$ are essentially the same for the two radicals, the canthaxanthin radical has an axial g-tensor (Table 1) in contrast to that in PSII which is rhombic. INDO molecular orbital calculations carried out by Knonovalova and co-workers indicate that canthaxanthin carbonyl groups carry no significant ground-state spin-density. This lack of oxygen spin-density is consistent with the relatively small g-anisotropy compared to pheophytins, semiquinones, and tyrosyl radicals, since the carbonyl group contribution to the g-tensor is scaled by the ground-state spin density on the oxygen.[22] Therefore, if the INDO accurately represent the ground-state singly occupied molecular orbital (SOMO), it is unlikely that the difference in g-values of the two carotenoids is due to the canthaxanthin carbonyl groups. To better understand the g-values of carotenoid radicals and obtain the orientation of tensor with respect to the molecular frame, we calculated the g-values of several polyenes based on the ZORA formalism as implemented in the Amsterdam Density Functional program package.[20,21] The results are shown in Table 2. First, the g-values of the polyene cation radical approach values which become independent of length. The differences between 6, 8, and 10 carbon chains are comparable to experimental limits. The effect of methyl groups and of cis−trans isomerization of the center bond are apparently negligible. As predicted by simple theory, the g_Z direction was perpendicular to the plane formed

by the polyene chain. The g_x direction was along the C−C single bonds. The g-values are in reasonable agreement with those measured by experiment. Overall the ZORA calculation overestimates the anisotropy contribution in the *x* and *y* direction by a factor of 2. It is clear that neither the calculations nor the theory predict an axially symmetric tensor.

The ZORA calculations of simple isolated polyene cationic radicals gave no indication of the source of the difference in g-tensors for β-carotene and canthaxanthin radicals. One difference between the radicals is their environment. In the case of the β-carotene, it is likely that it resides in a hydrophobic pocket within the protein. By comparison, canthaxanthin radical was generated on an activated, highly ionic silica−alumina surface. It is know that such molecules can interact strongly with this surface.[23] The very fact that a radical is spontaneously generated by exposure to the surface strongly indicates that molecule−surface interactions are significant. Hence, g-tensor of the canthaxanthin radical will likely reflect these interactions.

Hanley and co-workers[1] have reported the generation of stoichiometric amounts of $Car^{\bullet+}$ upon illumination at low temperature ($\leq$ 20 K). After the sample was incubated at higher temperatures (120−200 K) a conversion of $Car^{\bullet+}$ to $Chl_Z^{\bullet+}$ occurs in most of the centers and recombination in the remaining. These phenomena are also observed in the present experiments (Figure 1B to 1C). The signal intensity after the conversion from $Car^{\bullet+}$ to $Chl_Z^{\bullet+}$ dropped by about 20%. The resulting Chl_Z^{+} spectrum is identical in shape to the $Chl_Z^{\bullet+}$ generated by illumination at 198 K (Figure 1D). Since $Chl_Z^{\bullet+}$ is almost exclusively accumulated upon illumination at 120−198 K[1,4,2], the $Chl_Z^{\bullet+}$ obtained by conversion does not contain any significant amount of $Car^{\bullet+}$. This can be best seen at the low-field edge (dotted vertical line at $g = 2.00348$ in Figure 1), where the $Car^{\bullet+}$ absorbs in contrast to $Chl_Z^{\bullet+}$. Any significant contamination of $Car^{\bullet+}$ in the $Chl_Z^{\bullet+}$ spectrum would increase the absorption at the low-field edge.

Acknowledgment. We thank P. Dorlet for his advice in the preparation of the oriented samples and G. Voyard for technical assistance. This work was supported by grants from the Human Frontier Science Organization (Contract RGO249), from the EU through HCM FMRX-CT98-0214, and the Region Ile-de-France (Contract Sesame). P.F. was supported by grants from the Swiss National Science Foundation.

References and Notes

(1) Hanley, J.; Deligiannakis, Y.; Pascal, A.; Faller, P.; Rutherford, A. W. *Biochemistry* **1999**, *38*, 8189.

(2) Visser, J. W. M.; Rijgersberg, C. P.; Gast, P. *Biochim. Biophys. Acta* **1977**, *460*, 36.

(3) De Paula, J. C.; Innes, J. B.; Brudvig, G. W. *Biochemistry* **1985**, *24*, 8114.

(4) Deligiannakis, Y.; Hanley, J.; Rutherford, A. W. *J. Am. Chem. Soc*. **2000**, *122*, 400.

(5) MacMillan, F.; Rohrer, M.; Krzystek, J.; Brunel, L.-C.; Rutherford, A. W. *Photosynthesis: Mechanisms and Effects;* Garab, G, Ed.; Kluwer Academic Publisher: London, 1998; Vol. II, 715.

(6) Knonovalova, T. K.; Krzystek, J.; Bratt, P. J.; van Tol, J.; Brunel, L.-C.; Kispert, L. D. *J. Phys. Chem. B* **1999**, *103*, 5782.

(7) Plato, M.; Möbius, K. *Chem. Phys*. **1995**, *197*, 289.

(8) Bratt, P. J.; Poluektov, O. G.; Thurnauer, M. C.; Krzystek, J.; Brunel, L.-C.; Schrier, J.; Hsiao, Y.-W.; Zerner, M.; Angerhofer, A. *J. Phys. Chem. B.* **2000**, *104*, 6973−6977.

(9) Huber, M.; Törring, J. L. *Chem. Phys*. **1995**, *194*, 379.

(10) Stewart, D. H.; Cua, A.; Chisolm, A. D.; Diner, B. A.; Bocian, D. F.; Brudvig, G. W. *Biochemistry* **1998**, *37*, 10040.

(11) Koulougliotis, D.; Innes, J. B.; Brudvig, G. W. *Biochemistry* **1994**, *33*, 11814.

(12) Rigby, S. E. J.; Nugent, J. H. A.; O'Malley, P. J. *Biochemistry* **1994**, *33*, 10043.

(13) Un, S.; Brunel, L.-C.; Brill, T. M.; Zimmermann, J.-L.; Rutherford, A. W. *Proc. Natl. Acad. Sci. U.S.A.* **1994**, *91*, 5262.

(14) Dorlet, P.; Rutherford, A. W.; Un, S. *Biochemistry*, **2000**, *39*, 7826.

(15) Berthold, D. A.; Babcock, G. T.; Yocum, C. F. *FEBS Lett*. **1981**, *134*, 231.

(16) Ford, R. C.; Evans, M. C. W. *FEBS Lett.* **1983**, *160*, 159.

(17) Ivancich, A.; Mattioli, T. A.; Un, S. *J. Am. Chem. Soc*. **1999**, *121*, 5743.

(18) Press, W. H.; Flannery, B. P.; Teukolsky, S. A.; Vetterling, W. T. *Numerical Recipes*, 1986, Cambridge University Press: New York.

(19) Stewart, J. J. P. MOPAC, A Semiempirical Molecular Orbital Program, QCPE, *455*, 1983.

(20) (a)Amsterdam Denisty Functional Program Package, version ADF1999.02. (b) Baerends, E. J.; Ellis, D. E.; Ros, P. *Chem. Phys.* **1973**, *2*, 41. (c) Versluis, L.; Ziegler, T. *J. Chem. Phys*. **1988**, *322*, 88. (d) te Velde, G.; Baerends, E. J. *J Comput. Phys*. **1992**, *99*, 84. (e) Fonseca Guerra, C.; Snijders, J. G.; te Velde, G.; Baerends, E. J. *Theor. Chem. Acc*. **1998**, *99*, 391.

(21) van Lenthe, E.; Snijders, J. G.; Baerends, E. J. *J. Chem. Phys*. **1996**, *105*, 6505.

(22) (a) Stone, A. J. *Proc. R. Soc. A* **1963**, *271*, 424. (b) Stone, A. J. *Mol. Phys.* **1963**, *6*, 509. (c) Stone, A. J. *Mol. Phys.* **1964**, *7*, 311.

(23) See for instance: Ramamurthy, V.; Caspar, J. V.; Corbin, D. R. *J. Am. Chem. Soc.* **1991**, *113*, 594.